

HALO MONITOR FOR HIGH-INTENSITY HADRON BEAMS BASED ON SUPERSONIC GAS CURTAIN

H. Zhang ^{*}, W. Butcher, N. Kumar, F. Mada-Parambil, M. Patel, O. Sedlacek, S. Sethi, O. Stringer, C. Welsch, University of Liverpool / Cockcroft Institute, Daresbury, Warrington, UK

Abstract

In this contribution, a supersonic gas curtain-based profile monitor is considered for beam halo measurement in high-intensity, high-power hadron accelerators. This monitor is based on the beam gas curtain (BGC), successfully used in the Large Hadron Collider. Instead of a broad curtain with uniform density, a new concept with two shorter curtain segments that can be adapted to the shape of the beam core and aimed at only the halo particles is applied. The design and operation principle of the monitor will be presented, and the anticipated integration time, signal intensity, and dynamic range will be discussed, as well as opportunities to increase the sensitivity by incorporating microchannel plates or the Timepix detector.

INTRODUCTION

Although there is no clear definition of beam halo in particle accelerators [1], it is generally regarded as particles outside of the beam core with an intensity level lower than 10^{-4} or 10^{-6} of the peaks. In high-intensity, high-power hadron accelerators, halo particles may cause emittance growth and beam loss, difficulties in beam control and collimation, increase the noise of detectors and cause activation or even damage to accelerator components.

There are many theories and simulations for the formation of halos in the accelerator due to collective effects and space charge. To test these, experimental studies are essential. Due to the presence of the beam core, halo detection requires a dynamic range at least higher than 10^4 which is very challenging and few methods can meet the required high dynamic range. In the past, there have been several efforts towards the detection of the beam halo. Allen [2] used a combination of wire scanner and scrapper for the Low Energy Demonstration Accelerator (LEDA) which showed a dynamic range of 10^4 . Others used imaging techniques, such as charged injection device [3], coronagraphy [4] and adaptive masking [5] that showed a higher dynamics range of more than 10^4 , but these results need further investigation and their applications to major facilities are still lacking.

In this study, a gas curtain based halo monitor is considered. The monitor will detect the signal from the interaction of the halo particles and the gas molecule. To maintain a good vacuum condition, control the gas flow in a designed way and increase the local gas density, a supersonic gas curtain will be introduced. A similar gas curtain system has been successfully installed in the LHC [6] to detect the beam profile using the fluorescence generated from the interaction between the gas molecule and the charged particle beam.

To detect the beam halo, the fluorescence process no longer provides an adequate signal level and thus a higher cross-section process, such as impact ionisation will be chosen. We will discuss the principle of detection, the generation of gas curtains, the current experimental study using a laboratory electron source and a possible solution for beam halo detection for the LHC as an example.

GAS CURTAIN GENERATION FOR HALO DETECTION

Similar to the gas curtain used for the beam profile monitor [7], the supersonic molecular beam will be generated through a nozzle-skimmer system. A test setup was shown as Fig. 1. High-pressure gas flows through a $30\text{ }\mu\text{m}$ nozzle to the low-pressure nozzle chamber to form a supersonic gas jet. Two consecutive skimmers collimate the jet to form a molecular beam while creating differential pumping stages to maintain the background pressure at a low level. The first skimmer is a conical shape with $400\text{ }\mu\text{m}$ diameter. The second skimmer is a metal plate with a round hole opening. The radius was chosen as 2 mm and can be replaced with a larger size to generate broader beams. These two skimmers separate the vacuum vessel into a nozzle chamber, skimmer I chamber and skimmer II chamber. All chambers are pumped by separate sets of pumps. The number density of the molecular beam will drop gradually after the first skimmer because of a geometric expansion. A third skimmer was used to generate the gas curtain of a specific shape for diagnostic purposes. The shape can be very flexible. For example, for the beam profile monitoring, the third skimmer will be a 45° titled slit and the curtain will be similar to a screen which allows for 2D profile measurement. As for the halo detection, the interaction of the beam core with the gas curtain is avoided by generating two segments of curtains and leaving the molecular beam blank in the centre as shown in the enlarged area in Fig. 1. A metal plate with two segments of the slits is introduced for the 3rd skimmer as shown in Fig. 2. For test purposes, the gap was set as 4 mm and each slit has a geometry of $0.4\text{ mm} \times 10\text{ mm}$.

To estimate the density distribution of the gas curtain generated for halo detection, simulation and experimental study were performed and the results are shown in Fig. 3. To simplify the measurement, the 3rd skimmer was installed with both slits orientated 90° . The simulation is based on the quitting surface model for the transition from the continuum flow to molecular flow. The gas jet parameters in the continuum flow can be calculated directly according to the mass and energy conservation law. The particle ray tracing can be used to simulate the molecular flow part. The ex-

^{*} haozhang@liverpool.ac.uk

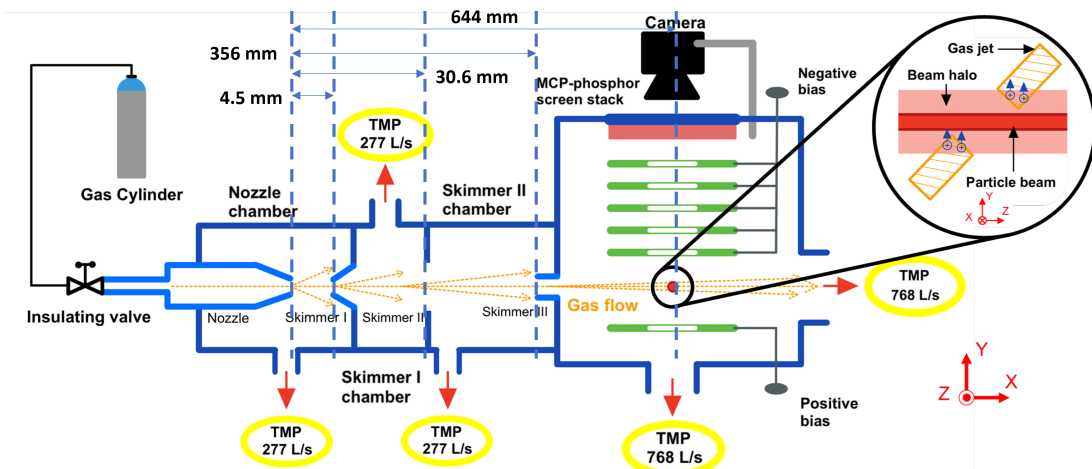


Figure 1: Principle of a gas-jet-based beam profile monitor [8].

perimental measurement used a scanning gauge method [9]. The simulated sub-curtain is about $0.8 \text{ mm} \times 16.8 \text{ mm}$ and the gap is about 7.2 mm . The measured sub-curtain is about $1.2 \text{ mm} \times 14.8 \text{ mm}$ and the gap is about 6.4 mm . For the width of the curtain, the measurement is larger which is due to the finite size of the pinhole of the movable gauge which is 1 mm . The measured distribution will be a convolution of the real distribution and the pinhole size. However, this will have little effect on the measurement of the length of the sub-curtain and the gap since they are much larger. The simulated lengths seem larger than the measured ones which might be due to the overestimation of the transverse velocity spread in the quitting surface model. The maximum number density is about 10 times higher in the simulation than in the experiment. The discrepancy in the number density arises from the challenge of accounting for all factors that attenuate the supersonic jet and the later molecular beam. Addressing this would require a detailed study incorporating both continuum and molecular flow simulations. Previous experience shows an empirical factor could apply to correct this difference. While quantification of the absolute density requires extensive study, the similarity of the shape between the simulation and measurement of the gas curtain density distribution will allow us to quickly iterate the design of the gas curtain such as the length, thickness and gap which can be tailored to the beam with different core sizes. There are large gaps between skimmer II, skimmer III and the interaction point. All these gaps can be reduced if higher-density curtains are required. Using the monitor used in the LHC with a compact design as an example, the number density can reach more than $1 \times 10^{16} \text{ m}^{-3}$.

EXPERIMENT TEST WITH THE ELECTRON BEAM

With the current gas curtain, the proof of principle measurement was performed by using a laboratory electron source with an energy of 5 keV which is shown in Fig. 4. In the experiments, the 3rd skimmer was orientated such that

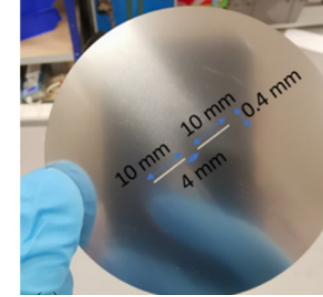


Figure 2: The picture of the 3rd skimmer

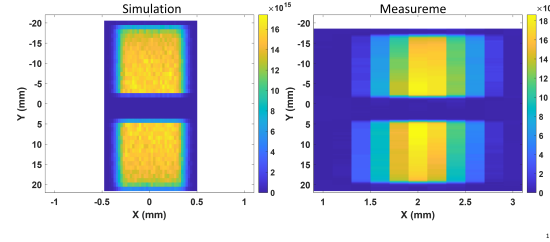


Figure 3: Number density distribution of the gas curtain in simulation, convolution and experiment.

the generated curtain is parallel to the beam propagation. This was intended to give another independent measurement of the curtain distribution initially. The ions generated from the interaction between the electron beam and gas curtain will be guided by an external electric field toward the micro-channel plates and CMOS camera. Notice that the electron beam will also ionise the residual gas, forming a continuous vertical line in the detector. Due to the directional velocity of the molecules in the supersonic gas curtain, the signal from the gas curtain will drift in the direction of the gas flow within the collection time, which depends on the external field and gas velocity. This velocity is about 780 m/s for the nitrogen supersonic gas curtain. The image in Fig. 4(a) again shows a distribution of the gas curtain. In the measurement, the electron beam is not able to cover the whole curtain even in the defocusing mode. Instead, a composition of multiple

measurements with different deflection angles of the electron beam gives a representation of the entire jet curtain. From the image, the feature of the sub-curtain can be seen and the size of the sub-curtain is about $1.5 \text{ mm} \times 13.6 \text{ mm}$ and the gap is about 5.5 mm . The difference of lengths in the electron beam measurement is due to the distortion from the extraction electric field which has a focus or defocus component. This was verified through a WARP simulation of the collection process which is shown in Fig. 5 and the details were explained in [8]. Note that the velocity spread of the gas curtain will be much smaller than the residual gas, the generated ions from the gas curtain will not expand that much compared with the ones from the residual gas.

Figure 4(b) demonstrates a case of halo measurement with a much smaller beam. Although the sub-curtains were orientated horizontally, the guided field could bend the electron beam so that the core would pass through the gap of the gas curtain. The one-dimensional tails are captured by the two sub-curtains. Because of the separation of the signal from the residual gas and supersonic gas curtain, we can measure the beam core (residual) and the halo at the same time. From the signal of the gas curtain, a clear masked area can be seen.

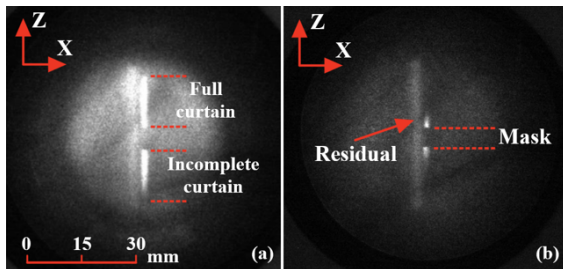


Figure 4: Measurement using the halo curtain with a low energy electron beam [8].

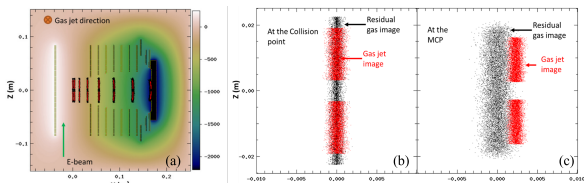


Figure 5: Simulation of ion collecting process under the external field for ions from the gas jet and the residual gas [8].

DISCUSSION

An important parameter for halo detection is the dynamic range of the measuring system. Due to the signal level and invasive feature, this monitor cannot perform a single-shot measurement which is a level of ms. Instead, it will give an average measurement or at least an integration time of seconds or even minutes. Theoretically, if the separation of the signals from the residual gas and gas curtain is present which means a slow collection time set by the external collecting field and no other fields distort the image, the dynamic range

will not be affected by the the beam core. It will only be limited by the size of the gap and the signal level from the ionisation between the beam halo and the gas curtain. This is an advantage of this method, compared with optical halo methods where the diffraction of the beam core will cause an issue. However, in realistic cases for ionisation beam profile monitor previously, a short collecting time was always set by the external field trying to lower the effect from the space charge distortion due to the primary beam, and then the two signals will overlap and the dynamic range will be decided by the intensity difference between the residual gas and the gas curtain. Currently, the number density of the gas curtain can reach $\sim 2 \times 10^{16} \text{ m}^{-3}$ while keeping the background gas density at a level of $\sim 1 \times 10^{-8} \text{ mbar}$ or $2.4 \times 10^{14} \text{ m}^{-3}$, which means in the worst scenario, a dynamic range is about 10^2 . To increase the dynamic range, either the gas curtain density must be increased or a better background pressure must be maintained. To increase the gas curtain density, a compact design can be adapted to reduce the distance from the nozzle to the interaction point. The background pressure can be improved by increasing the pumping speed. Furthermore, the collection process with both residual signal and gas curtain signal can be studied by simulations with different external fields in the presence of space charge. Due to the properties of directionality and cold temperature for the supersonic gas curtain, if the slow collection can be applied, the separation of the signals can be improved thereby improving the dynamic range.

CONCLUSION

In summary, a halo monitor based on a supersonic gas curtain and ionisation beam profile monitor was proposed. A special curtain shape with two sub-curtains for halo measurement and a gap for blocking the beam core was realised by a special skimmer design. The number density distribution of such curtain was demonstrated in both simulation and experiment, which shows similarity in its shape, an important parameter in the context of the profile measurement. It will allow us to tailor the halo monitor for different core sizes by modifying the skimmer design. A proof of principle measurement was done using a low-energy electron beam. The potential dynamic range was discussed and in the worst scenario, it can be 10^2 . Further investigation for the ion collection process needs to be studied where a suitable collecting time is set by the external field to trade off the separation of the signals and the resolution lost due to space charge distortion. In this way, the dynamic range could be much improved.

ACKNOWLEDGEMENT

This work was supported by the STFC Cockcroft core grant No. ST/G008248/1.

REFERENCES

[1] K. Wittenburg, “Overview of recent halo diagnosis and non-destructive beam profile monitoring”, in *Proc. HB’06*,

Tsukuba, Japan, May-Jun. 2006, pp. 54–58, 2006. <https://jacow.org/abdwlb06/papers/TUAZ01.pdf>.

[2] C. K. Allen *et al.*, “Beam-halo measurements in high-current proton beams”, *Phys. Rev. Lett.*, vol. 89, no. 21, p. 214802, 2002. doi:10.1103/PhysRevLett.89.214802

[3] C. P. Welsch, E. Bravin, B. Burel, T. Lefèvre, T. Chapman, and M. J. Pilon, “Alternative techniques for beam halo measurements”, *Meas. Sci. Tech.*, vol. 17, no. 7, pp. 2035–2040, 2006. doi:10.1088/0957-0233/17/7/050

[4] T. Mitsuhashi, “Beam Halo Observation by Coronagraph”, in *Proc. DIPAC'05*, Lyon, France, Jun. 2005, pp. 7–11. <https://jacow.org/d05/papers/ITMM03.pdf>.

[5] H. D. Zhang, R. B. Fiorito, A. G. Shkvarunets, R. A. Kishek, and C. P. Welsch, “Beam halo imaging with a digital optical mask”, *Phys. Rev. Spec. Top. Accel. Beams*, vol. 15, no. 7, p. 072803, 2012. doi:10.1103/PhysRevSTAB.15.072803

[6] H. Zhang *et al.*, “BGC monitor: first year of operation at the LHC”, presented at IBIC'24, Beijing, China, Sep. 2024, paper FRAC2, this conference.

[7] A. Salehilashkajani *et al.*, “A gas curtain beam profile monitor using beam induced fluorescence for high intensity charged particle beams”, *Appl. Phys. Lett.*, vol. 120, no. 17, p. 174101, 2022. doi:10.1063/5.0085491

[8] O. Stringer, N. Kumar, C. P. Welsch, and H. D. Zhang, “A Gas Jet Beam Halo Monitor for LINACs”, in *Proc. LINAC'22*, Liverpool, UK, pp. 227–230, 2022. doi:10.18429/JACoW-LINAC2022-MOPORI04

[9] H. Zhang, A. Salehilashkajani, O. Sedlacek, and C. Welsch, “Characterization of a supersonic molecular beam for charged particle beam profile monitor”, *Vacuum*, vol. 208, p. 111701, 2023. doi:10.1016/j.vacuum.2022.111701